XI International Conference on Computational Plasticity. Fundamentals and Applications
COMPLAS XI
E. Oñate, D.R.J. Owen, D. Peric and B. Suárez (Eds)

3D MODELLING OF GEOMATERIALS ACCOUNTING FOR AN UNCONVENTIONAL PLASTICITY APPROACH

VALENTINA A. SALOMONI*, RICCARDO FINCATO*

* Department of Structural and Transportation Engineering
Faculty of Engineering, University of Padua
Via F.Marzolo, 9 – 35131 Padua, Italy
e-mail: salomoni@dic.unipd.it, fincato@dic.unipd.it, www.dic.unipd.it

Key words: Coupled problems, Compaction, Subsidence, Plasticity, Subloading surface.

Abstract. The coupled hydro-mechanical state in geomaterials undergoing plasticity phenomena is here evaluated by means of the subloading surface model . The most important feature of this theory is the abolition of the distinction between the elastic and plastic domain, as it happens in conventional elastoplastic models. This means that plastic deformations are generated whenever there is a change in stress and a smoother elasto-plastic transition is produced. The subloading surface takes the role of a loading surface which always passes through the current stress point $\boldsymbol{\sigma}$ and keeps a shape similar to that of the normal yield surface and a similar orientation with respect to the origin of stress space. Additionally, the model allows for giving a smooth response in a smooth monotonic loading process and the stress is automatically drawn back to the normal-yield surface even if it goes out from that surface, leading to a more stable and robust calculation even for large loading steps. The plasticity algorithm has been implemented within the FE PLASCON3D research code, coupling hydro-(thermo)-mechanical fields within a saturated porous medium (locally partially saturated) subjected to external loads. Applications to soils allow e.g. for assessing subsidence evolution at regional scale.

1 INTRODUCTION

The three-dimensional behaviour of geomaterials is here analysed making specifically reference to soils undergoing compaction and ensuing surface subsidence due to gas withdrawal from a typical deep reservoir.

Surface subsidence due to withdrawal of underground fluids occurs in many parts of the world, see for instance the case book of Poland [1]. Such surface settlement is a particular threat if it is experienced in low lying areas, close to the sea. Surface subsidence of this kind is almost exclusively understood in terms of drop of pressure in the aquifers or in the reservoir: i.e. withdrawal of these underground fluids results in a reduction of their pressure downhole; this in turn increases the part of the overburden carried by the skeleton of the reservoir rocks causing compaction. The compaction manifests itself, through deformation of the overlying strata, as surface settlement.

In case of a single fluid (water) involved, compaction can easily be explained by the principle of Terzaghi [2] which states that the compression of a porous medium is controlled by changes of effective stresses, i.e. variations of the difference between total stresses and the pressure of the fluid in the pores. However, when more fluids are involved or more phases of the same fluid, the Terzaghi traditional expression of effective stress alone is not sufficient to completely justify measured compaction and the concepts of unsaturated soil mechanics with appropriate stress measures and elastoplasticity concepts are needed. Drop of reservoir pressure is not the only mechanism leading to reservoir compaction and suction effects must also be accounted for at least for some types of extracted fluids and some reservoir rocks.

Capillary effects and structural collapse are treated in [3]-[5] and seem to provide sound explanations for continuing surface settlements when reservoir pore pressures stabilise and for additional settlements occurring even after the end of gas production. However, it is to be said that for the investigated area here considered, undergoing subsidence, there is no direct experimental evidence on samples from the field to show the key effect of capillarity on subsidence itself and hence any additional consideration could be largely speculative with many assumptions that are not justified enough.

Again, the discussion about the contribution of capillary effects when performing reservoir compaction and subsidence analyses at regional scale is out of scope for the present paper. The idea is to make use of unconventional plasticity [6] by means of the subloading surface model [7]-[11] for predicting softening behaviour of soil as well as reducing computational efforts when performing fully coupled hydro-mechanical subsidence analyses in three-dimensional domains [12], as demonstrated below.

It is to be said that, from a computational point of view, strain-softening may be associated to numerical procedures affected by a lack of convergence and the solution may depend strongly on the mesh adopted. Several techniques have been reported in literature, essentially when dealing with shear band formation and strain localization [13], [14], employed to obtain mesh size-independent shear banding (e.g. [15]). Mesh size-dependent hardening modulus procedures have been proposed by Pietruszczak and Mroz [16] and employed by a number of authors (e.g. Willam [17], Grammatikopoulou et al. [18]); enrichments or enhancements of the continuum models can be alternatively found [19]-[26] which include the non-local

formulation proposed by Eringen [27] and Kroner [28] and developed extensively by Bažant and Cedolin [29]. A complete review of softening plasticity models with internal variables regularized by non-local averaging of integral type can be found in Marotti de Sciarra [30], where it is stated that the appropriate choice of the regularization operator and of the internal variables to model a non-local continuum need to be dealt with a combination of micromechanical analysis and experimental investigations; probably only experimental investigations can provide the validation of one choice or of the other.

However, as evidenced in Yamakawa et al. [31], the accuracy and the convergence property of the subloading surface model (even if there incorporated into a stress-update algorithm for the Cam-Clay one), when e.g. used to reproduce over-consolidated soils experiencing softening, has been demonstrated for a single finite element and a plane mesh of 2460 8-node quadratic elements as well; in the latter situation different mesh sizes have not been considered. The robustness of the model has been there proved by increasing the number of loading steps only, even when considering dilation with a decrease in deviatoric stress.

Hence at present, essentially considering the main objectives of this paper as outlined before and in line with [31], it seems reasonable to prove the accuracy of the calculations presented here by comparing the numerical solutions for different mesh sizes and time steps as well; such a comparison is developed in the last Section, referring to the 3D subsidence analysis on regional scale.

2 FLOW FIELD ANALYSIS

It is here made reference to the coupled solution proposed in [32]-[36] to obtain the flow data necessary for a compaction analysis. This solution considers the mass balance equation in integral form for the fluids in the reservoir, which is then solved together with the state equation of gas via a three-dimensional consolidation analyzer, which uses an (a) equilibrium equation for the multiphase medium (solid + water or solid + gas) and a (b) mass balance equation for the water; the code has been upgraded to take into account possible plastic strain evolutions, following an unconventional plasticity approach, as exposed in the next Section.

The material balance equation referring to the reservoir and the state equation of gas yield at each time step the average reservoir pressure p_g when gas production and water inflow are known; this gas pressure is applied to the reservoir volume and the whole subsiding volume is then analysed by using the fully coupled equations (a) and (b). These equations give the flow of water across the reservoir boundary which is required in the material balance equation at reservoir level, and also its deformation, as well as of the overburden and underburden.

The reader is referred to [36]-[37] for additional details.

3 MODELLING PLASTICITY VIA THE SUBLOADING SURFACE MODEL

The subloading surface model is a particular elasto-plastic model falling within the framework of unconventional elastoplasticity [6], an extended elastoplasticity theory such that the interior of the yield surface is not a purely elastic domain, but rather a plastic deformation is induced by the rate of stress inside the yield surface [7]-[11]. Its main features are briefly

recalled here.

In the subloading surface model the conventional yield surface is renamed the *normal yield surface*, since its interior is not regarded as a purely elastic domain. The plastic deformation develops gradually as the stress approaches the normal yield surface, exhibiting a smooth elastic-plastic transition. Thus the subloading surface model fulfils the *smoothness condition* [11], [39]-[41], which is defined as the stress rate-strain rate relation (or the stiffness tensor) changing continuously for a continuous change of stress rate. Strain accumulation is predicted for a cyclic loading with an arbitrary stress amplitude, where the magnitude of accumulated strain depends continuously on the stress amplitude because of the fulfillment of the smoothness condition. Inelastic deformation occurs immediately when the stress point once again moves outward the current yield surface. Zero diameter yield surface bounding surface models, nested surface models, and subloading models have this attribute, but do not display any purely elastic response [6].

A *subloading surface* is also introduced, which always passes through the current stress point $\boldsymbol{\sigma}$ and keeps a shape similar to that of the normal yield surface and a similar orientation with respect to the origin of stress space, i.e. $\boldsymbol{\sigma} = \mathbf{0}$.

The ratio of similarity R is named *normal yield ratio* and governs the approach of the subloading surface to the normal one, i.e. if R = 0 the subloading surface is a point coinciding with the origin of the stress space, whereas $0 < R < 1$ represents the subyield state and with R = 1 the stress lies directly on the normal surface.

The subloading surface can be described by the scalar-valued tensor function

$$f(\boldsymbol{\sigma}) = RF(H) \tag{1}$$

where the scalar H is the isotropic hardening/softening variable; in agreement with [10] the normal yield surface takes e.g. the form

$$F = F_0 \exp\left(\frac{H}{\rho' - \gamma}\right) \tag{2}$$

in which F_0 is the initial value of F, ρ' and γ the slopes of the normal consolidation and swelling curves respectively in $\ln\upsilon$-$\ln p$ space (υ being the specific volume and $p = -\mathrm{tr}(\boldsymbol{\sigma})/3$).

The extended consistency condition for the subloading surface is obtained by differentiating Eq. (1), which leads to

$$\mathrm{tr}\left(\frac{\partial f(\boldsymbol{\sigma})}{\partial \boldsymbol{\sigma}}\dot{\boldsymbol{\sigma}}\right) = \dot{R}F + RF'\dot{H} \tag{3}$$

together with considering the evolution rule of the normal yield ratio, given by

$$\dot{R} = U\left\|\dot{\boldsymbol{\varepsilon}}^{p}\right\| \quad \text{for} \quad \dot{\boldsymbol{\varepsilon}}^{p} \neq \mathbf{0} \tag{4}$$

where $\dot{\boldsymbol{\sigma}}$ is the proper objective co-rotational stress rate, $\dot{\boldsymbol{\varepsilon}}^{e} = \mathbf{E}^{-1}\dot{\boldsymbol{\sigma}}$, $\dot{\boldsymbol{\varepsilon}}^{p}$ is the plastic strain rate

and U is a monotonically decreasing function of R satisfying the condition

$$\begin{cases} U = +\infty \quad \text{for} \quad R = 0 \\ U = 0 \quad \text{for} \quad R = 1 \\ (U < 0 \quad \text{for} \quad R > 1) \end{cases} \tag{5}$$

The associated flow rule is assumed as

$$\dot{\boldsymbol{\varepsilon}}^{\mathrm{p}} = \overline{\lambda}\,\overline{\mathbf{N}} \tag{6}$$

where $\overline{\lambda}$ is the positive proportional factor representing the increment of plastic deformation along the direction given by the normalized outward normal of the subloading surface $\overline{\mathbf{N}}$ (expressed as a second order tensor)

$$\overline{\lambda} = \frac{\mathrm{tr}\,(\overline{\mathbf{N}}\dot{\boldsymbol{\sigma}})}{\overline{\mathrm{M}}^{\mathrm{p}}} \tag{7}$$

$$\overline{\mathbf{N}} \equiv \frac{\partial \mathrm{f}(\boldsymbol{\sigma})}{\partial \boldsymbol{\sigma}} \Bigg/ \left\| \frac{\partial \mathrm{f}(\boldsymbol{\sigma})}{\partial \boldsymbol{\sigma}} \right\| \tag{8}$$

being $\overline{\mathrm{M}}^{\mathrm{p}}$ the plastic modulus.

The loading criterion is finally given [41], [42]

$$\begin{cases} \dot{\boldsymbol{\varepsilon}}^{\mathrm{p}} \neq \mathbf{0}: \quad \mathrm{tr}\,(\overline{\mathbf{N}}\mathbf{E}\dot{\boldsymbol{\varepsilon}}) > 0 \\ \dot{\boldsymbol{\varepsilon}}^{\mathrm{p}} = \mathbf{0}: \quad \mathrm{tr}\,(\overline{\mathbf{N}}\mathbf{E}\dot{\boldsymbol{\varepsilon}}) \leq 0 \end{cases} \tag{9}$$

For additional details, see [37], [38].

4 APPLICATION CASE: 3D SUBSIDENCE ANALYSIS ON REGIONAL SCALE

The numerical model has been first calibrated and subsequently validated against the results obtained by Siriwardane and Desai [43], the first dealing with the consolidation of a column of soil under a uniformly distributed load, the second with the consolidation of a soil strip in plane strain. For brevity reasons, the procedures and their results are not reported here; they have anyway allowed for defining a value for the plastic variables necessary to the subloading surface model (see below) so to reproduce the same behaviour as the one evidenced in [43] accounting for conventional plasticity.

It is additionally to be said, as previously stated, that the main objective here is not to compare the material response by assuming conventional or unconventional plasticity models (about which it has been largely discussed in e.g. [40], [41]) but, on one side, to numerically confirm the capability of the subloading surface model in predicting softening behaviours and, on the other side, to be able to explain, via such a model, ongoing surface subsidence

(observed in reality) after shutdown of the wells. In fact, it has already been proved in [4] that conventional plasticity alone is not fully able to reproduce such a phenomenon.

A typical subsidence problem of regional scale is here investigated, referring to a pools' depth of burial ranging between 900 and 4000 m and an horizontal area involved of about 19000 Km^2 (**Figure 1**). In addition, the different pools are not scheduled to be put in production at the same time, which complicates the situation further.

Figure 1: Location of gas pools in the Northern Adriatic Sea [44].

Particularly, the effects of the exploitation of four of the gas reservoirs shown in **Figure 1**, located at three different depths and undergoing different production histories [45], are here analysed; the region covers an area of 40×40 km^2 and has a depth of 1300 m; it is discretized by about 500 20-node isoparametric elements (additional analyses, as reported below, refer to 980 and 2940 elements as well). Free flux on the horizontal and vertical boundaries of the investigated area is considered. The main material parameters are shown in **Table 1** [35], [45]; the grains are assumed to be incompressible and the clayey layers to behave in agreement with the subloading surface model when accounting for plasticity effects. The geomechanical data have been obtained through analysis of master-logs at our disposal, which are representative of the investigated area, whereas the plastic variables have been taken from the calibration and validation tests, appropriately scaled to take into account the effect of depth.

As evidenced by **Table 1** and **Figure 2**, some planimetric variability for the soil strata has been additionally introduced just to be closer to the real configuration of the subsoil, e.g. considering the available seismic section of [45]; so 7 *macro-levels* are present, including 15 different soil strata. The exploitation points (wells) are assumed to be equally distributed above each reservoir such as to allow for the assumption of a constant drop of pressure inside them.

The analysis has been pushed up to 30 years from the beginning of exploitations, when a general pressure recovery has already been attained; the results in terms of surface subsidence above each reservoir are shown in **Figure 3**, accounting for elasticity and unconventional elasto-plasticity as well. The effect of interaction among the different reservoirs can be seen from the shifting in time of the maximum subsidence value as compared with the minimum of reservoir pressure: this phenomenon is also to be partly ascribed to the presence of clay layers

confining the pools, but it is particularly evident when plasticity is introduced: as an extreme situation, maximum subsidence can not be reached even after 30 years; a "residual" delayed land subsidence has clearly appeared, so confirming the usefulness of the proposed unconventional plasticity model for modelling continuing surface settlements when reservoir pore pressures stabilize and for additional settlements occurring even after the end of gas production.

Table 1: Material data for subsidence analyses

Soil stratum #	**E** [MPa]	ν	$\mathbf{k_i}$ [m/day]	**Depths [m]**
1	$1.13 \cdot 10^4$	0.17	0.2208	1300÷1254
2	$1.00 \cdot 10^4$	0.17	$0.865 \cdot 10^{-4}$	1300÷1254
3 & Reservoir # 1	$1.13 \cdot 10^4$	0.17	0.2208	1300÷1254
4	$1.00 \cdot 10^4$	0.17	$0.865 \cdot 10^{-4}$	1300÷1254 & 1300÷1070
5, 7, 9	$1.14 \cdot 10^4$	0.30	0.7985	1254÷1070
6, 8, 10	$0.322 \cdot 10^4$	0.38	$0.865 \cdot 10^{-4}$	1254÷1070
11 & Reservoir # 4	$1.14 \cdot 10^4$	0.30	0.7985	1070÷1027
12	$0.322 \cdot 10^4$	0.38	$0.865 \cdot 10^{-4}$	1027÷860
13 & Reservoirs # 2, 3	$0.898 \cdot 10^4$	0.15	0.9752	860÷848
14	$0.555 \cdot 10^4$	0.37	$0.865 \cdot 10^{-4}$	848÷600
15	$0.224 \cdot 10^4$	0.39	$0.865 \cdot 10^{-4}$	600÷0

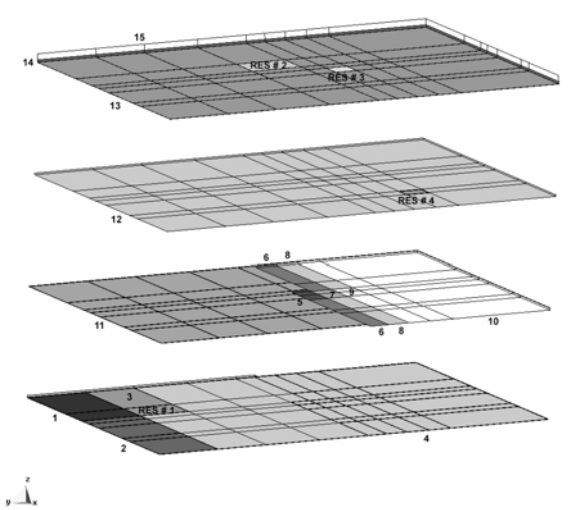

Figure 2: Schematic representation of the soil strata distribution: macro-levels are superimposed from surface (top) to bottom (see **Table 1**).

The subsidence bowl is depicted in **Figure 4**, referring to the evolution of surface subsidence for a fixed domain section when unconventional plasticity is accounted for. The time scales involved, as well as the orders of magnitude for the resulting subsidence, agree well with what evidenced by [45] and [46] (the former referring to linear elasticity only), with similar (or equal, as in the latter case) cumulative gas production histories and geological/geomechanical subsoil configurations.

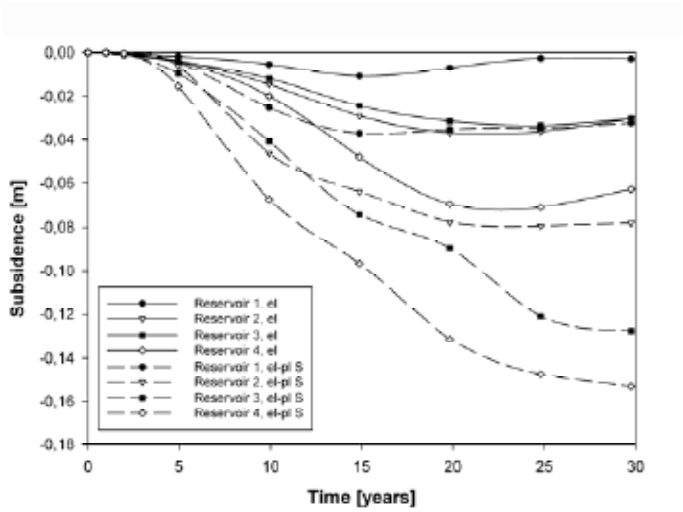

Figure 3: History of surface subsidence above the reservoirs.

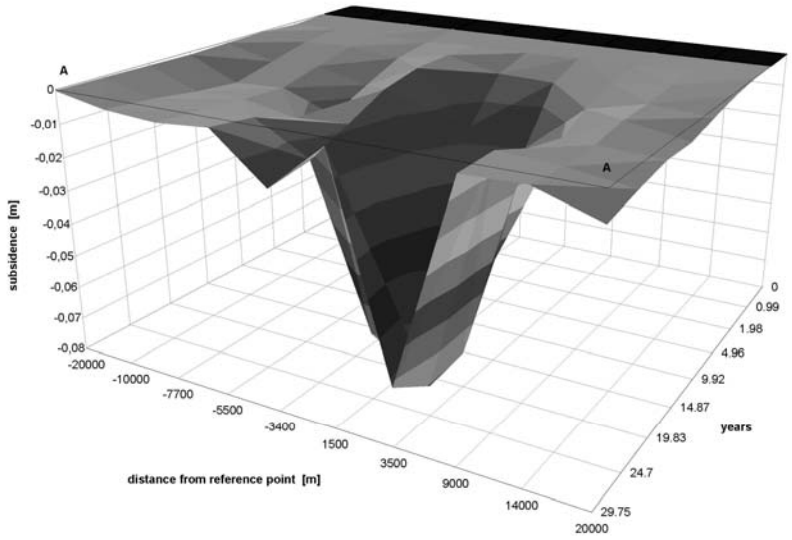

Figure 4: Subsidence bowl, elasto-plastic case.

In order to check the robustness of the model, a series of additional numerical analyses has been performed, by assuming a) different time (loading) steps, and b) different mesh sizes; the results refer to unconventional plasticity analyses only. In the former situation, three reference time-steps have been accounted for, i.e. 362 (load-case LS1), 181 (LS2) and 90.5 days (LS3) respectively (for additional details the reader is referred to [38]): an independence of the computations on loading steps has been clearly evidenced. Two reference points (RP1 close to the deepest rigid underburden, belonging to layer 4 -see **Table 1-**, and RP2, at about 1100 m depth and at the conjunction of layers 6-9 and under layer 12, both in proximity of Reservoir

1) have been considered for representing stress-strain curves (**Figure 5**) taking into account LS1 and LS2 only (being the results of LS3 superimposed to those of LS2): after a short expansion phase, the soils evidence or hardening or softening, depending on material characteristics and depth; the smoothness and shape of the elasto-plastic curves (subloading model) recalls the one reported in [10]. Elastic responses have been added for comparison purposes only. It is to be noticed that the unloading phases do not occur simultaneously with pressure recovery (of e.g. Reservoir # 1) but they are delayed in time. The mechanisms are strongly differentiated depending on the considered points, but they can give a general estimate of the complexity of the subsoil behaviour and they can provide for a first explanation of observed delayed surface settlements.

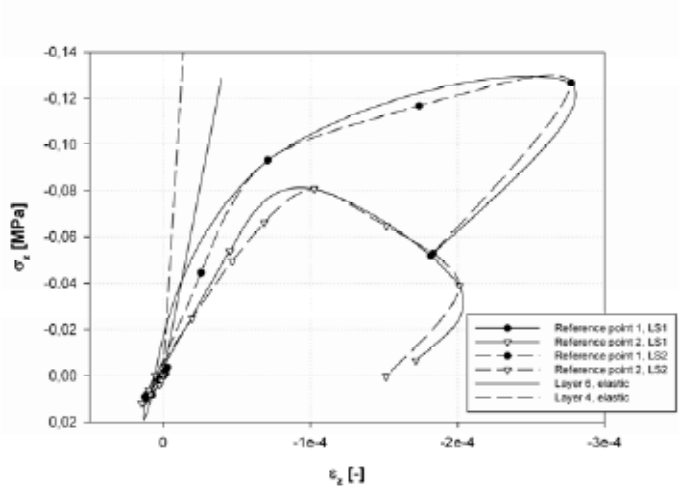

Figure 5: Stress-strain curves for RP1 and RP2.

To complete the check of the plasticity model, two additional meshes have been considered [38]: 4907 nodes and 980 20-node isoparametric elements (M1) and 13978 nodes and 2940 20-node isoparametric elements (M2), with 5 d.o.f. (u_i, i = 1-3, p, T) per node as for the first mesh (M0) of **Figure 1**. The results are depicted in **Figure 6** in terms only of surface subsidence for sake of brevity, referring to the elasto-plastic results from the load-case LS1: mesh independency is evidenced, with a maximum error (taking as reference the values from M2) of about 10%: the error tends to decrease with time, suggesting the ability of the model to perform long-term predictive subsidence analyses.

5 CONCLUSIONS

The coupled hydro-mechanical state in soils coming from consolidation/subsidence processes and undergoing plasticity phenomena has been evaluated by means of the subloading surface model, allowing for predicting a smooth response for smooth monotonic loading, considering the sign of $\mathrm{tr}(\overline{\mathbf{N}}\mathbf{E}\mathbf{D})$ only in the loading criterion, automatically drawing back of a stress to the normal yield surface even if it goes out from the surface itself. Hence a

rough numerical calculation with a large loading step is allowed and return-mapping iterative techniques can subsequently be skipped, so enhancing speedup and efficiency of large scale coupled analyses, as required when modelling subsidence in 3D domains and for long-term scenarios. The plasticity algorithm has been implemented in the PLASCON3D FE code, coupling hydro-thermo-mechanical fields within a saturated (locally partially saturated) porous medium subjected to external loads and water/gas withdrawals from deep layers (aquifers/reservoirs).

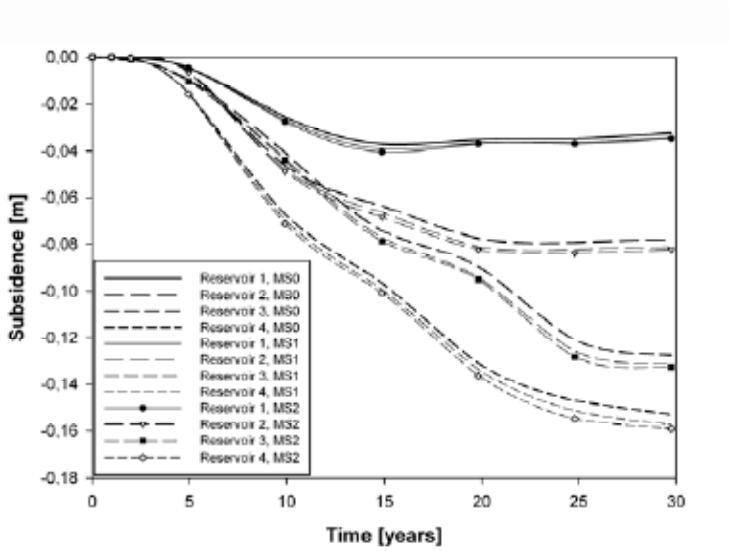

Figure 6: Surface subsidence above the reservoirs, unconventional elasto-plasticity analyses; mesh sizes M0, M1, M2.

The plastic deformation due to the change of stress inside the yield surface exhibiting a smooth elastic-plastic transition has been described, as well as a first ability of describing softening behaviours has been shown.

The robustness of the model has been tested by comparing numerical solutions for different mesh sizes and different time steps.

Regional subsidence analyses due to gas extractions have been possible with reduced computational efforts when introducing unconventional elasto-plasticity in the code. It has been demonstrated that the time scales involved, as well as the orders of magnitude for the resulting subsidence, agree well with what evidenced by [45] and [46] (the former referring to linear elasticity only), with similar (or equal, as in the latter case) cumulative gas production histories and geological/geomechanical subsoil configurations. Particularly, the effects of interaction among exploitations have been estimated, as well as the phenomenon of residual land subsidence near abandoned gas fields has been successfully modelled: the estimation of this delayed environmental cost of gas pumping is generally neglected, whereas it clearly appears of being fundamental for an increased awareness of the consequence that gas production may have on future coastline stability relatively far from the gas field [46].

REFERENCES

[1] Poland, J. (Ed.). *Guidebook to Studies of Land Subsidence due to Groundwater withdrawal*. UNESCO, Paris (1984).

[2] Terzaghi, K. Die Berechnung der Durchlassigkeitsziffer des Tones aus dem Verlauf der hydrodynamischen Spannungserscheinungen. *Akademie der Wissenchaften in Wien, Sitzungsberichte, Mathematisch-naturwissenschaftliche Klasse*, Part Iia (1923) **132**(3/4): 125-138.

[3] Schrefler, B.A., Bolzon, G., Salomoni, V., Simoni, L. On compaction in gas reservoirs. *Atti dell'Accademia Nazionale dei Lincei - Rendiconti Lincei: Scienze Fisiche e Naturali*, s. IX (1997) **VIII**(4): 235-248.

[4] Simoni, L., Salomoni, V., Schrefler, B.A. Elastoplastic subsidence models with and without capillary effects. *Comp. Meth. Appl. Mech. Engrg*. (1999) **171**(3-4): 491-502.

[5] Menin, A., Salomoni, V.A., Santagiuliana, R., Simoni, L., Gens A, Schrefler BA. A mechanism contributing to subsidence above gas reservoirs. *Int. J. Comp. Meth. Engrg. Sci. Mech*. (2008) **9**(5): 270-287.

[6] Drucker, D.C. Conventional and unconventional plastic response and representation. *J. Appl. Mech. Rev.* ASME (1988) **41**(4):151-167.

[7] Hashiguchi, K., Ueno, M. Elastoplastic constitutive laws of granular materials. *Proc. 9th Int. Conf. Soil Mech. Found. Engrg*. Special Session 9, Tokyo, Japan (1977): 73-82.

[8] Hashiguchi, K. Constitutive equations of elastoplastic materials with elastic-plastic transitions. *ASME J. Appl. Mech*. (1980) **47**(2): 266-272.

[9] Hashiguchi, K. Subloading surface model in unconventional plasticity. *Int. J. Solids Struct.* (1989) **25**(8): 917-945.

[10] Hashiguchi, K., Saitoh K, Okayasu T, Tsutsumi S. Evaluation of typical conventional and unconventional plasticity models for prediction of softening behaviour of soils. *Geotech*. (2002) **52**(8): 561-578.

[11] Hashiguchi, K. *Elastoplasticity theory*. In: F Pfeiffer, P Wriggers (Eds.), Lecture notes in applied and computational mechanics. Springer: Berlin (2009) **42**: 393 p.

[12] Yale, D.P. Coupled geomechanics-fluid flow modelling: effects of plasticity and permeability alteration. *SPE/ISRM Rock Mech. Conf*. Irving, TX, USA, Oct. 20-23 (2002) **SPE/ISRM 78202**: 10 p.

[13] Needleman, A. Material rate dependence and mesh sensitivity in localization problems. *Com. Meth. Appl. Mech. Engrg.* (1988) **67**: 69-86.

[14] Garikipati, K., Hughes, T.J.R. A study of strain localization in a multiple scale framework - the one dimensional problem. *Com. Meth. Appl. Mech. Engrg.* (1998) **159**: 193-222.

[15] Zhou, H., Randolph, M.F. Computational Techniques and Shear Band Development for Cylindrical and Spherical Penetrometers in Strain-Softening Clay. *Int. J. Geomech.* (2007) **7**(4): 287-295.

[16] Pietruszczak, S., Mroz, Z. Finite element analysis of deformation of strain softening materials. *Int. J. Num. Meth. Engrg.* (1981) **17**: 327-334.

[17] Willam, K. *Experimental and computational aspects of concrete failure*. In: F. Damjanic (Ed.), Computer Aided Analysis and Design of Concrete Failure. Pineridge Press: Swansea (1984): 33-70.

[18] Grammatikopoulou, A., Zdravkovic, L., Potts, D.M. General Formulation of Two Kinematic Hardening Constitutive Models with a Smooth Elastoplastic Transition. *Int. J. Geomech.* (2006) **6**(5): 291-302.

[19] Aifantis, E.C. On the microstructural origin of certain inelastic models. *J. Engrg. Mat. Tech.* (1984) **106**: 326-334.

[20] Pijaudier-Cabot, G., Bažant, Z.P. Nonlocal damage theory. *ASCE J. Engrg. Mech.* (1987) **113**(10): 1521-1533.

[21] Mühlhaus, H.B., Vardoulakis, I. The thickness of shear bands in granular materials. *Geotech.* (1987) **37**: 271-283.

[22] Bažant, Z.P., Lin, F.B. Non-local yield limit degradation. *Int. J. Num. Meth. Engrg.* (1988) **26**: 1805-1823.

[23] Mühlhaus, H.B., Aifantis, E.C. A variational principle for gradient plasticity. *Int. J. Solids Struct.* (1991) **28**: 845-857.

[24] De Borst, R., Mühlhaus, H.B. Gradient dependent plasticity: formulation and algorithmic aspects. *Int. J. Num. Meth. Engrg.* (1992) **35**: 521-539.
[25] De Borst, R., Sluys, L.J., Mühlhaus, H.B., Pamin, J. Fundamental issues in finite element analyses of localization of deformation. *Engrg. Comp.* (1993) **10**: 99-121.
[26] Galavi, V., Schweiger, H.F. Nonlocal Multilaminate Model for Strain Softening Analysis. *Int. J. Geomech.* (2010) **10**(1): 30-44.
[27] Eringen, A.C. Theory of micropolar continuum. *Proc. 9th Midwestern Mechanical Conference*. University of Wisconsin, Madison, Wisconsin (1965): 23-40.
[28] Kroner, E. Elasticity theory of material with long-range cohesive forces. *Int. J. Solids Struct.* (1967) **3**:731-742.
[29] Bažant, Z.P., Cedolin, L. *Stability of Structures*. Oxford University Press: NY (1991).
[30] Marotti de Sciarra, F. A general theory for nonlocal softening plasticity of integral-type. *Int. J. Plasticity* (2008) **24**: 1411-1439.
[31] Yamakawa, Y., Hashiguchi, K., Ikeda, K. Implicit stress-update algorithm for isotropic Cam-clay model based on the subloading surface concept at finite strains. *Int. J. Plasticity* (2010) **26**(5): 634-658.
[32] Lewis, R.W., Schrefler, B.A. *A finite element simulation of the subsidence of gas reservoirs undergoing a waterdrive*. In: RH Gallagher, DH Norrie, JT Oden, OC Zienkiewicz (Eds.), Finite Element in Fluids. Wiley: Chichester (1982) **4**: 179-199.
[33] Schrefler, B.A., Lewis, R.W., Majorana, C.E. Subsidence above volumetric and waterdrive gas reservoirs. *Int. J. Num. Meth. Fluids* (1981) **1**(2): 101-15.
[34] Lewis, R.W., Schrefler, B.A. *The finite element method in the deformation and consolidation of porous media*. Wiley: Chichester (1987).
[35] Lewis, R.W., Schrefler, B.A. *The finite element method in the static and dynamic deformation and consolidation of porous media*. Wiley: Chichester (1998).
[36] Schrefler, B.A., Wang, X., Salomoni, V., Zuccolo, G. An efficient parallel algorithm for three-dimensional analysis of subsidence above gas reservoirs. *Int. J. Num. Meth. Fluids* (1999) **31**(1): 247-60.
[37] Salomoni, V.A., Fincato, R. 3D subsidence analyses above gas reservoirs accounting for an unconventional plasticity model. *Int. J. Num. Anal. Meth. Geomech*. (2011) (in press).
[38] Salomoni, V.A., Fincato, R. Subloading surface plasticity model algorithm for 3D subsidence analyses above gas reservoirs. *Int. J. Geomech*. (2011) (in press).
[39] Hashiguchi, K. Mechanical requirements and structures of cyclic plasticity models. *Int. J. Plasticity* (1993) **9**(6): 721-748.
[40] Hashiguchi, K. The extended flow rule in plasticity. *Int. J. Plasticity* (1997) **13**(1): 37-58.
[41] Hashiguchi, K. Fundamentals in constitutive equation: continuity and smoothness conditions and loading criterion. *Soils Found*. (2000) **40**(3): 155-161.
[42] Hashiguchi, K. On the loading criterion. *Int. J. Plasticity* (1994) **10**(8): 871-878.
[43] Siriwardane, H.J., Desai, C.S. Two numerical schemes for non linear consolidation, *Int. J. Num Meth. Engrg.* (1981) **17**: 405-426.
[44] *Il Sole 24 Ore*, July 16 (2008) **195** (in Italian).
[45] AGIP, *Progetto Alto Adriatico – Studio di impatto ambientale*. AGIP, San Donato, Italy (1996) (in Italian).
[46] Baù, D., Gambolati, G., Teatini, P. Residual land subsidence near abandoned gas fields raises concern over Northern Adriatic coastland. *Eos* (2000) **81**(22): 245-249.